

Sequential-segment multi-shot auto-calibration for GRAPPA EPI: maximizing temporal SNR and reducing motion sensitivity

Jonathan R. Polimeni¹, Himanshu Bhat², Thomas Benner³, Thorsten Feiweier³, Souheil J. Inati⁴, Thomas Witzel¹, Keith Heberlein², and Lawrence L. Wald^{1,5}

¹A.A. Martinos Center for Biomedical Imaging, Department of Radiology, Harvard Medical School, Massachusetts General Hospital, Charlestown, MA, United States,

²Siemens Medical Solutions USA Inc., Charlestown, MA, United States, ³Siemens AG, Healthcare Sector, Erlangen, Bavaria, Germany, ⁴National Institute of Mental Health, Bethesda, MD, United States, ⁵Harvard-MIT Division of Health Sciences and Technology, MIT, Cambridge, MA, United States

Target audience: Clinicians/researchers using accelerated echo planar imaging, especially in high-field or high-resolution applications.

Purpose: In accelerated parallel imaging echo planar imaging (EPI) acquisitions, GRAPPA auto-calibration signals (ACS) are ideally matched to the echo spacing of the image data to ensure equivalent distortion. To accomplish this, a multi-shot or segmented EPI acquisition is employed for the ACS acquisition. To prevent slice cross-talk in multi-slice acquisitions, the segmented reference lines are acquired in a slice-interleaved manner. This approach imposes a full TR interval between adjacent segments in *k*-space, making the method vulnerable to patient movement or respiration-induced dynamic B_0 changes. Furthermore, time-series SNR is intermittently reduced and discontinuous SNR across adjacent slices is possible, which may lead to a spatial detection bias for even- or odd-numbered slices in fMRI studies. Here we introduce a new auto-calibration method based on acquiring multi-shot, multi-slice EPI where the multiple segments of the ACS acquisition are acquired sequentially in time for each slice. Because of the short recovery time between shots, the flip angle for each shot must be chosen to yield equal magnetization across the segments. Our revised strategy for ACS acquisition requires no modification of the image reconstruction algorithm and therefore provides a simple and effective method for improving image quality.

Methods: A conventional GRE-EPI pulse sequence was developed to implement novel acquisition strategies for the GRAPPA ACS data. For an image acquisition with acceleration factor R the sequential-segment multi-shot EPI ACS acquisition (**SeqSeg**) consisted of R shots, and each segment had the same echo spacing as the accelerated image acquisition. Both gradient and RF spoiling were used after each shot of the ACS acquisition to eliminate remaining transverse magnetization before the next pulse. The flip angles required to maintain equal magnetization across segments were: $45^\circ, 90^\circ$ for $R=2$; $35^\circ, 45^\circ, 90^\circ$ for $R=3$; $30^\circ, 35^\circ, 45^\circ, 90^\circ$ for $R=4$.^{1,2} Because the T_1 values vary across the brain, we also tested an ACS acquisition scheme based on the FLEET

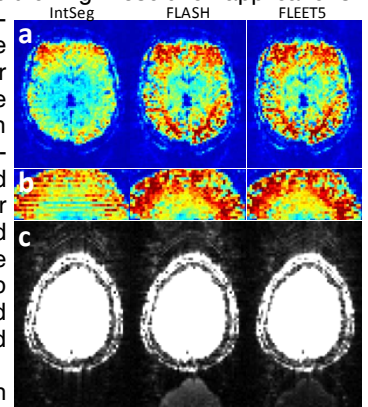


Fig. 1: (a) tSNR maps of $R=3$ GRAPPA reconstructions from three ACS acquisitions. (b) Sagittal reformats of tSNR maps. Note the discontinuous tSNR across slices in the IntSeg example. (c) Images after B_0 manipulation, windowed to highlight residual aliasing artifacts.

method³ in which the same, small flip angle (α) is used for each shot. We tested $\alpha=5^\circ$ (**FLEET5**) and $\alpha=20^\circ$ (**FLEET20**). The $\alpha=20^\circ$ scheme required five “dummy” RF pulses to establish equilibrium longitudinal magnetization. Four dummy pulses were played between the ACS and image acquisitions for the FLEET scans.

Three volunteers (having given informed consent) were scanned on a MAGNETOM Trio A Tim System 3-T whole-body scanner (Siemens AG, Healthcare Sector, Erlangen, Germany) using the manufacturer’s 32-channel coil. Subjects were instructed to remain still. We acquired $3 \times 3 \times 3$ mm³ EPI data with TE/TR/BW/matrix/fa/esp = 30 ms/2000 ms/2264 Hz/px/96/90/0.51 ms. We tested acceleration factors $R=2, 3$, and 4, and for each protocol the maximum number of reference lines were acquired. The time for each ACS shot was 23 ms, for a total ACS acquisition time of 46, 69 and 92 ms per slice for $R=2, 3$ and 4, respectively.

Time-series SNR (tSNR) was calculated as the time-series mean divided by the standard deviation after motion correction and linear detrending⁴. For comparison, conventional slice-interleaved single-shot (**1Seg**) and multi-shot (**IntSeg**) ACS lines were acquired, as well as ACS lines with a FLASH readout.⁵ To assess sensitivity to susceptibility distortions, additional scans were acquired where B_0 inhomogeneity was induced by manually offsetting the x gradient offset “shim” by 50 μ T/m. The ghost level was quantified from a ROI outside of the brain region (not including pixels containing the shifted fat layer). To assess the motion sensitivity, we repeated all scans on a motion phantom consisting of an anthropomorphic brain phantom⁶ undergoing continuous nodding motion around the R–L axis (pivoting on the bridge of the nose) driven continuously by motor throughout the scan, with a period of 15 s and a 5° extent of rotation.

Results: Example tSNR maps and the corresponding image reconstructions are shown in Fig. 1. The tSNR is comparable between the FLASH and FLEET5 ACS examples, however the IntSeg ACS exhibits discontinuous tSNR in the slice direction. In the data acquired with induced B_0 inhomogeneity, the ghost artifact (reflecting residual aliasing) is strongest in the FLASH ACS example due to echo spacing mismatch between the image and ACS data. Fig. 2 shows the motion sensitivity. As expected, there is a dramatic reduction in motion-induced residual aliasing artifact in the FLEET5 example because the shorter duration of the ACS acquisition for each slice. A summary of the tSNR and residual aliasing across the ACS schemes averaged over the three subjects is shown in Fig. 3. The tSNR values across acceleration rates are consistent with previously reported values.⁴ The FLEET5 ACS scheme resulted in the highest tSNR across the methods, although the tSNR was comparable to the FLASH and FLEET20 ACS data. The residual aliasing was also always lower in the FLEET5 ACS data compared to the FLASH, although the trend is small.

Discussion: The SNR of the FLEET ACS data itself is low due to the small flip angle, and thus its performance is expected to degrade with small-voxel acquisitions where SNR losses could impact the kernel fitting. In these cases the SeqSeg scheme, which employs a higher flip angle, may provide higher tSNR.

Conclusion: The sequential-segment multi-shot EPI ACS method provides higher tSNR and resilience to motion than the conventional approach while maintaining the echo spacing of the image data, providing low artifact levels in the presence of B_0 inhomogeneity. Also, the discontinuous SNR seen across slices in the conventional IntSeg scheme is successfully removed by the proposed method.

References: [1] Mansfield (1984) *MRM* 1:370. [2] Wang *et al.* (2005) *Proc ISMRM* 13:2409. [3] Chapman *et al.* (1987) *MRM* 5:246. [4] Triantafyllou *et al.* (2011) *NeuroImage* 55:597. [5] Griswold *et al.* (2006) *NMR in Biomed* 19:316. [6] Graedel *et al.* (2012) *Proc ISMRM* 20:314.

Acknowledgements: Supported by NIBIB K01-EB011498 and NCCR P41-RR14075. We thank K. Setsompop for helpful discussions.

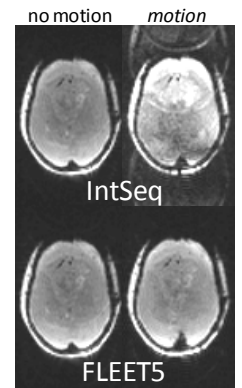


Fig. 2: Effect of motion.

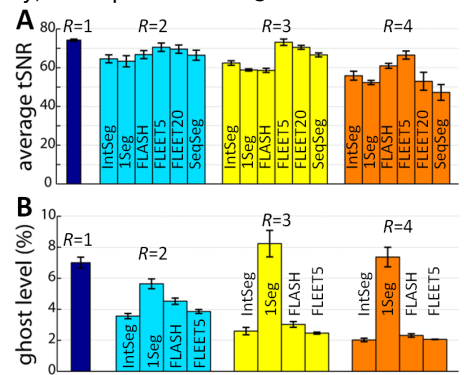


Fig. 3: Comparison of methods across subjects. (A) SNR for each ACS scheme. (B) Residual aliasing after B_0 manipulation.